

# Evolution of physical properties & scaling relations for high-redshift galaxies

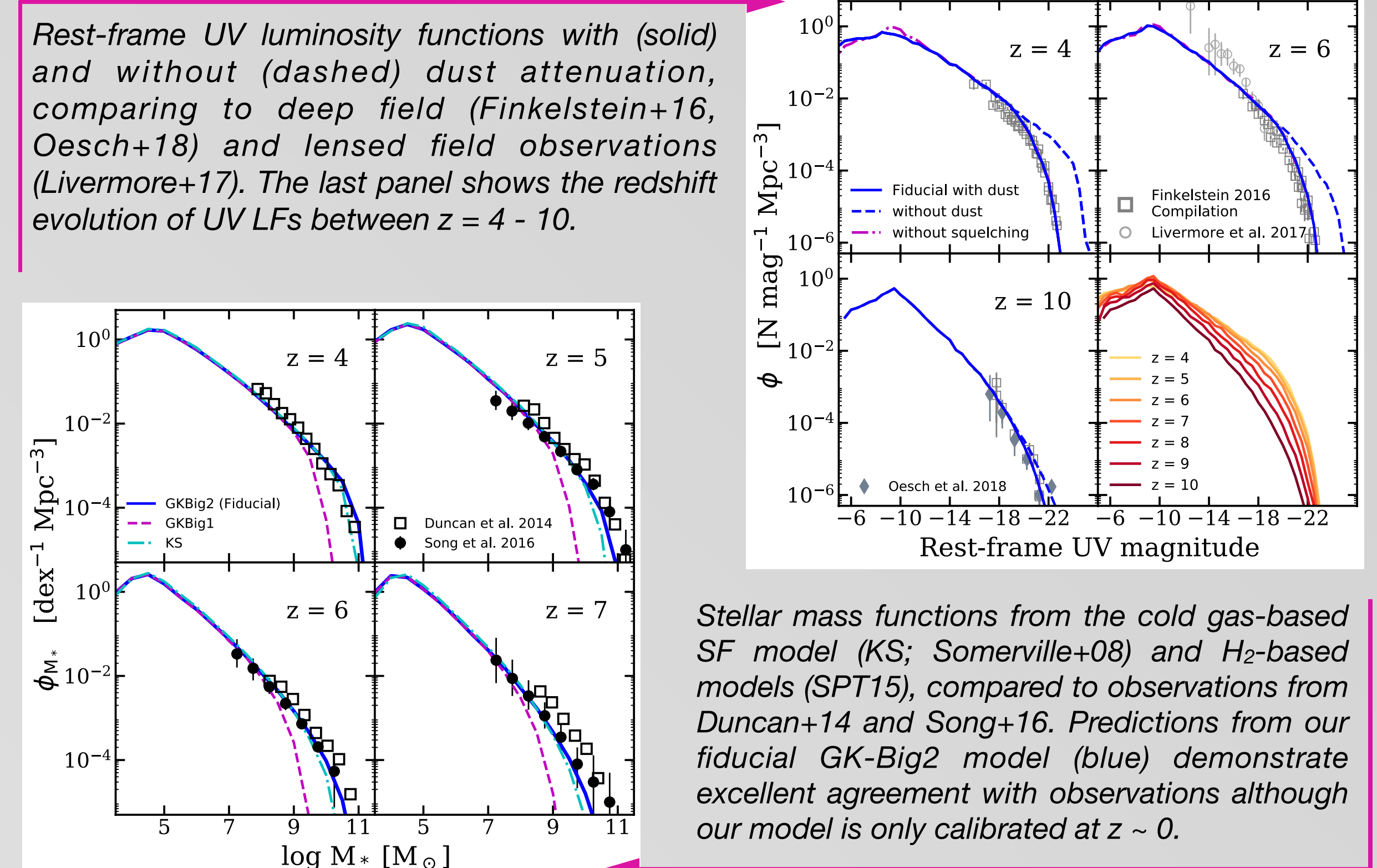
L. Y. Aaron Yung and Rachel S. Somerville

email: yung@physics.rutgers.edu

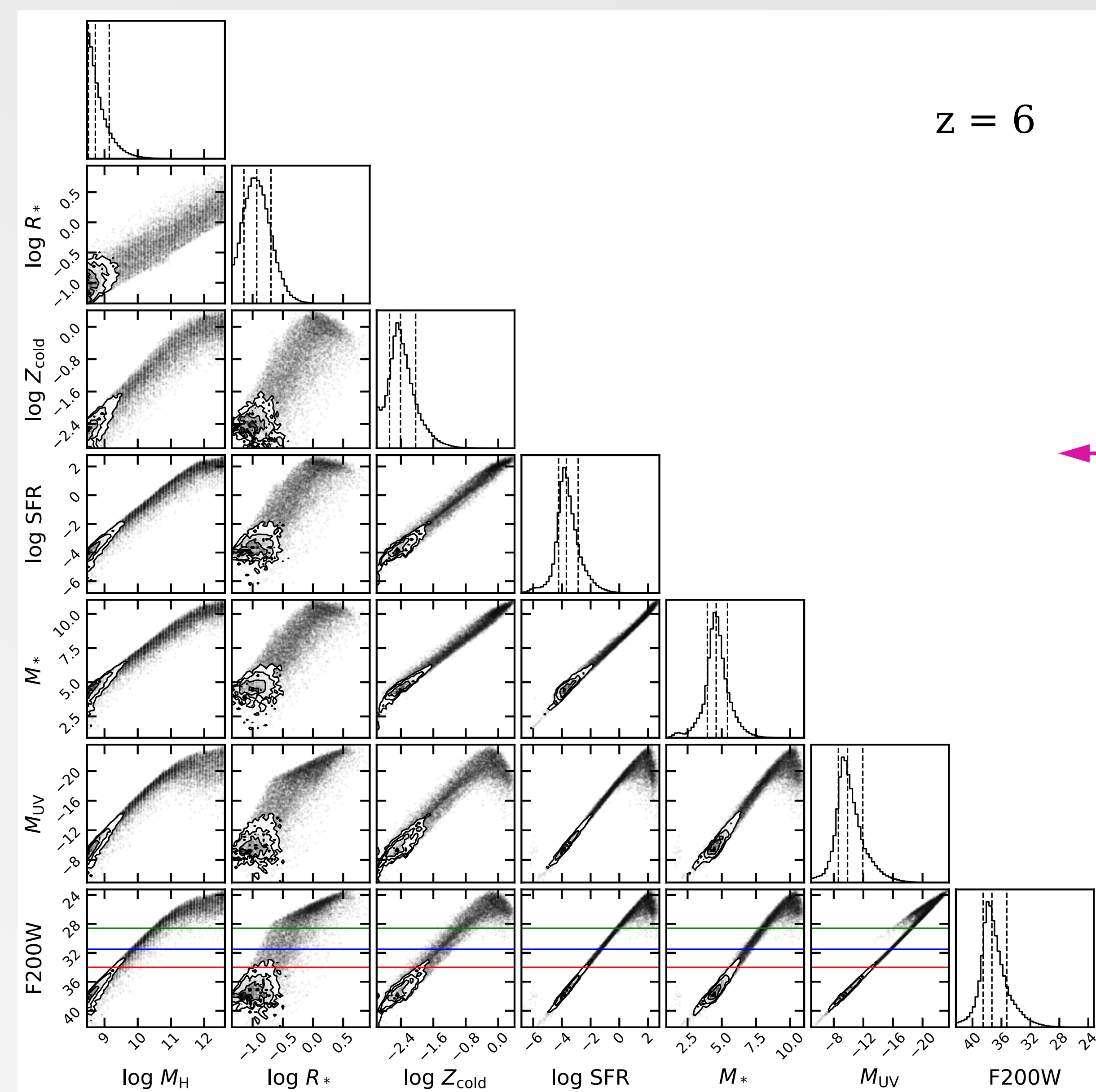
data: <http://www.physics.rutgers.edu/~yung/>

## The Santa Cruz semi-analytic model

- In anticipation of upcoming *JWST* observations, we present predictions for observable properties of high- $z$  galaxy populations ( $z = 4 - 10$ ). We utilize the well-established Santa Cruz semi-analytic model with the recently implemented multiphase gas partitioning and  $H_2$ -based star formation recipes (Somerville, Popping & Trager 2015). Our model can efficiently sample halos over a wide mass range, covering galaxies forming in atomic cooling halos to the most massive halos forming at these epochs.
- With free parameters in our model only calibrated to a subset of observations at  $z \sim 0$ , it is intriguing that our results agree so well with the existing observations across  $z \sim 4 - 8$ . Taking advantage of the SAM's high computational efficiency, we are also able to explore the sensitivities of high- $z$  galaxy properties to the uncertainties in the underlying physical processes by systematically varying the model free parameters and SF prescriptions. See [Paper I arXiv:1803.09761](#) for details and other results.



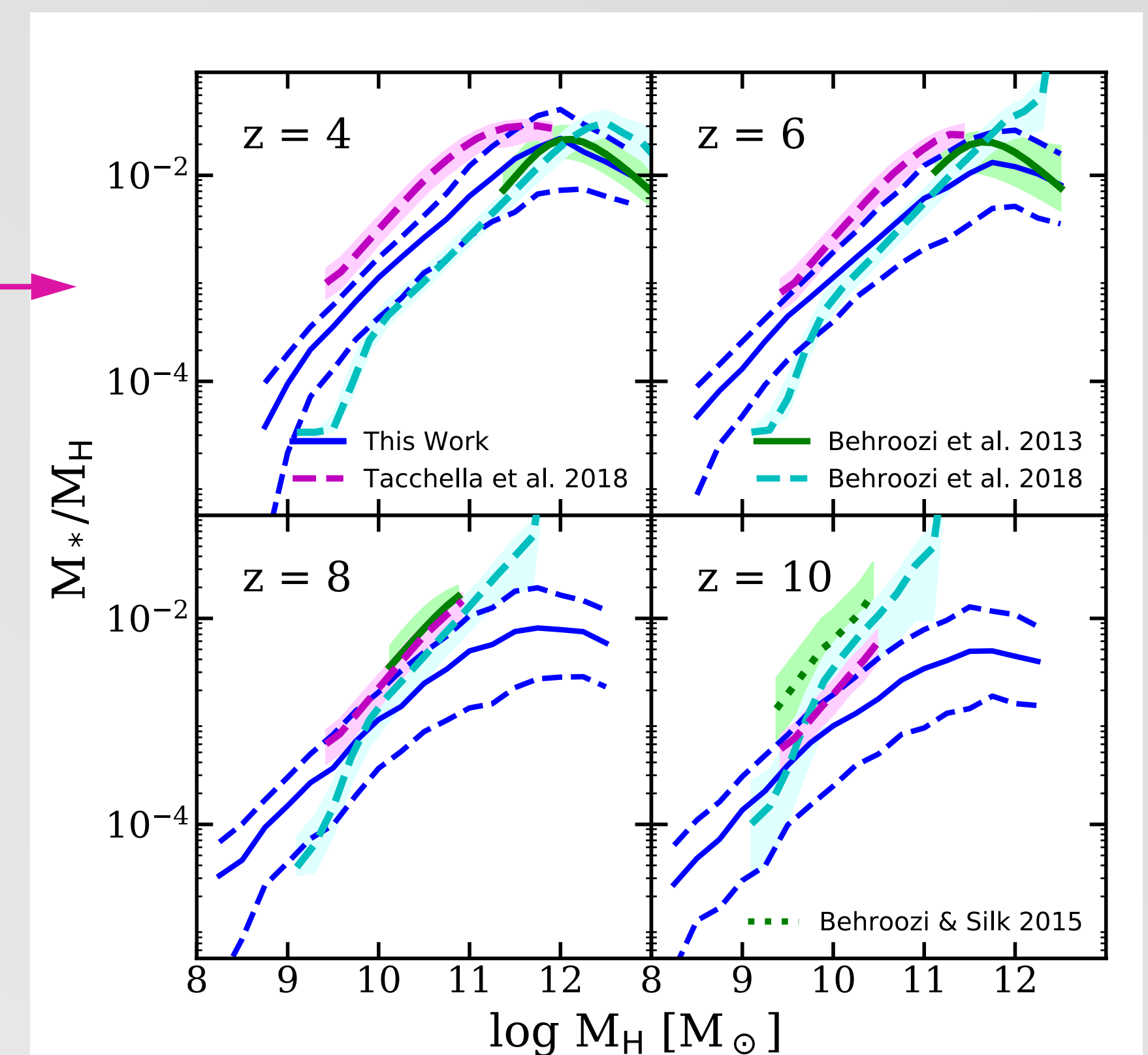
## Properties & Scaling Relations of high- $z$ galaxies



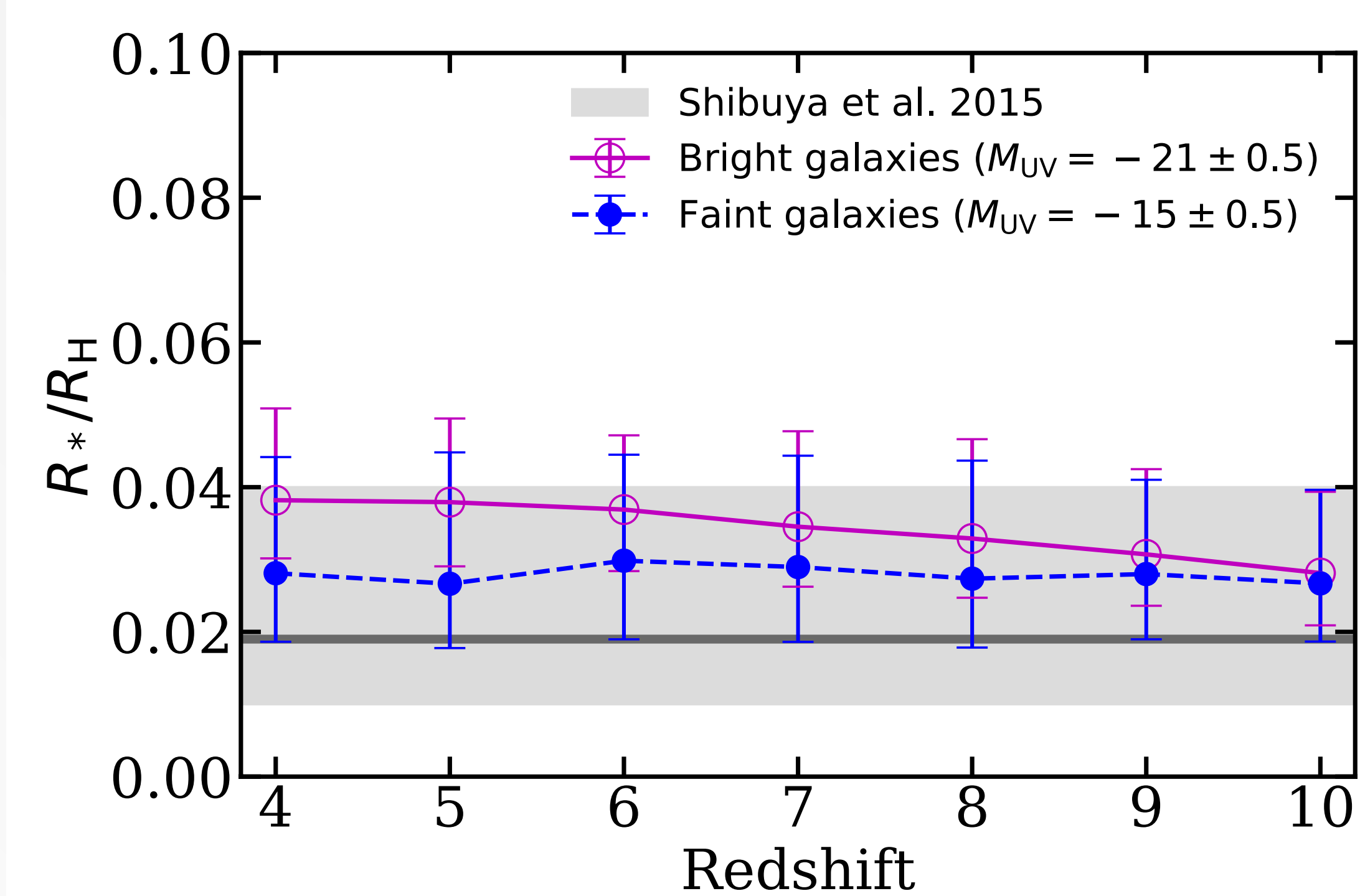
- Properties of galaxies at high redshifts remain largely unconstrained, and it is one of *JWST*'s primary goals to put additional observational constraints on these populations. We illustrate the demographics and properties of galaxy populations at high redshift predicted by our model. Here we present the correlation among selected physical properties at  $z = 6$ , including halo mass, stellar disc radius, cold gas metallicity, star formation rate, stellar mass, rest-frame UV luminosity with dust attenuation, and apparent magnitude calculated for the NIRCам F200W filter; all masses and metallicities are given in solar units, while the stellar radius is in kpc. The green, blue, and red horizontal lines mark the detection limits of mock wide-, deep-, and lensed-field survey, respectively. The contours in the scatter plot and the vertical lines in the histograms mark the 16th, 50th, and 84th percentile. Addition plots for  $z = 8$  and  $10$  are available online.

Look out for detailed analysis in the upcoming [Paper II](#).

- We show a comparison of the stellar-to-halo mass ratio from our model to abundance matching results from Behroozi+13 and analytic predictions from Behroozi & Silk '15, and the latest empirical models from Behroozi+18 and Tacchella+18. Upcoming *JWST* observations will distinguish between these models.



- The redshift evolution of stellar-to-halo size ratio predicted by our model, where the bright and faint galaxies are presented separately. The gray band approximates the abundance matching results presented by Shibuya+15 ( $z \sim 4 - 8$ ). The radius shown for our model is the 3D half-stellar mass radius, which is expected to be slightly larger than the projected, rest-UV effective radius measured by observations. It is intriguing that the rather simple relation adopted in our model is in good agreement with constraints out to  $z \sim 8$ .



- Here we showcase the predicted redshift evolution for the scaling relations among stellar mass ( $M^*$ ) a few key physical properties, including rest-frame UV luminosity ( $M_{UV}$ , with or without dust attenuation), star formation rate (SFR), specific star formation rate (SSFR), and cold gas metallicity ( $Z_{cold}$ ). These predictions are compared to the recently released results from two empirical models by Behroozi+18 and Tacchella+18. It is rather interesting that these model agree quite well at low redshifts but each evolve very differently toward high redshift. Upcoming *JWST* observations will be able to distinguish between these models.

